

Supporting Information for

**4- Trifluoromethoxyproline:
Synthesis of Stereoisomers and Lipophilicity Study**

Ivan G. Logvinenko,^{a,b} Iryna V. Sadkova,^a Nataliya A. Tolmachova,^a Svitlana V. Shishkina,^{c,d}
Constantin G. Daniliuc,^e Günter Haufe^{e,f} and Ivan S. Kondratov,^{*a,b,g}

^a *Enamine Ltd. (www.enamine.net), Winston Churchill Street 78, Kyiv 02094, Ukraine*

^b *V.P. Kukhar Institute of Bioorganic Chemistry & Petrochemistry, National Academy of Sciences of Ukraine, Academician Kukhar Str 1, Kyiv 02660, Ukraine*

^c *SSI "Institute for Single Crystals" of the National Academy of Sciences of Ukraine, Nauky Ave. 60, Kharkiv 61072, Ukraine*

^d *Institute of Organic Chemistry of the National Academy of Sciences of Ukraine, Academician Kukhar Str. 5, Kyiv 02660, Ukraine*

^e *Organisch-Chemisches Institut, Universität Münster, Corrensstraße 40, Münster 48149, Germany*

^f *Cells-in-Motion Cluster of Excellence, Universität Münster, Waldeyerstraße 15, 48149 Münster, Germany*

^g *Enamine Germany GmbH (www.enamine.de), Industriepark Hoechst, G837, 65926 Frankfurt am Main, Germany*

X-Ray analysis

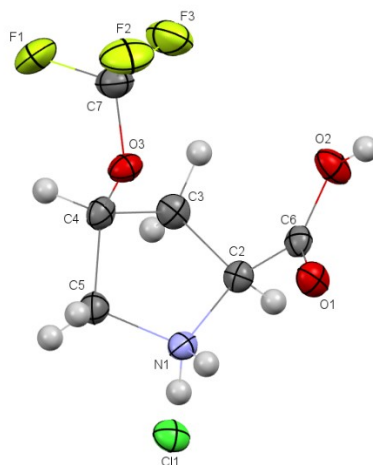


Figure S1. Molecular structure of compound **(2S,4S)-6-HCl** according to X-ray diffraction data. Thermal ellipsoids of non-hydrogen atoms are shown at 50% probability level.

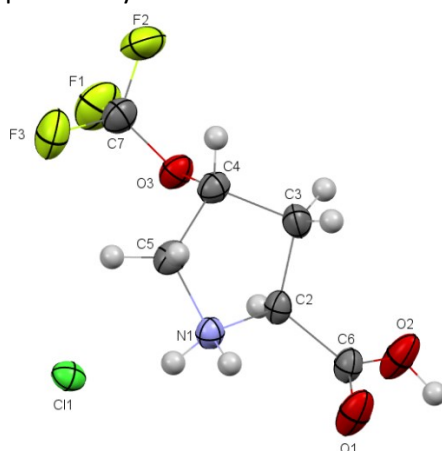


Figure S2. Molecular structure of compound **(2S,4R)-6-HCl** according to X-ray diffraction data. Thermal ellipsoids of non-hydrogen atoms are shown at 50% probability level.

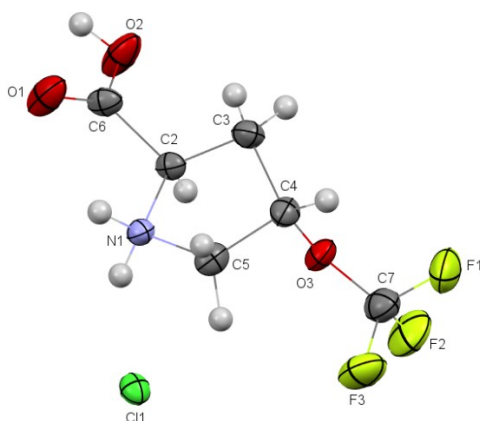


Figure S3. Molecular structure of compound **(2R,4S)-6-HCl** according to X-ray diffraction data. Thermal ellipsoids of non-hydrogen atoms are shown at 50% probability level.

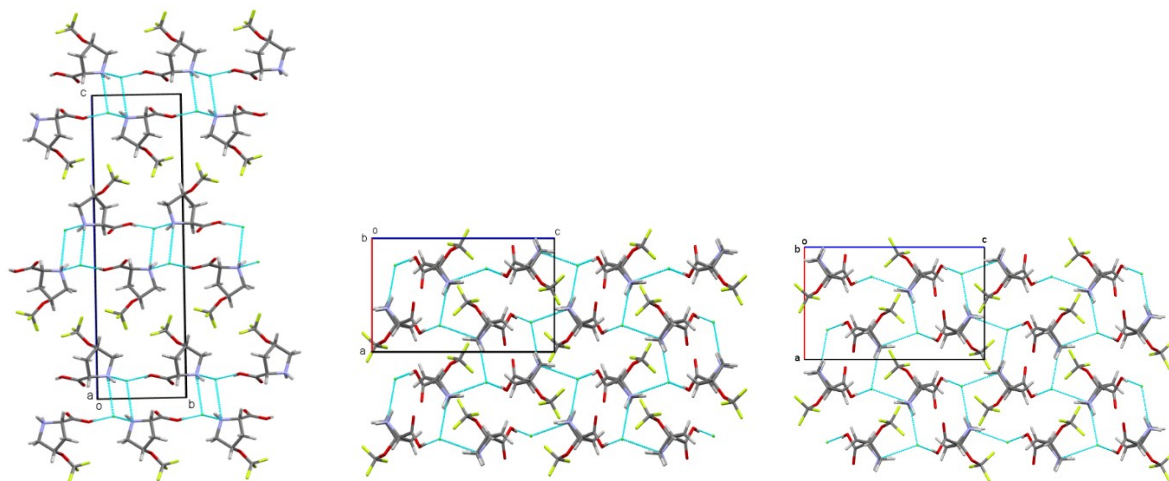


Figure S4. Packing molecules **(2S,4S)-6**, projection in the *c* crystallographic direction (on the left) and **(2S,4R)-6**, **(2R,4S)-6**, projection in the *b* crystallographic direction (in the middle and on the right). Hydrogen bonds are shown in blue dashed lines.

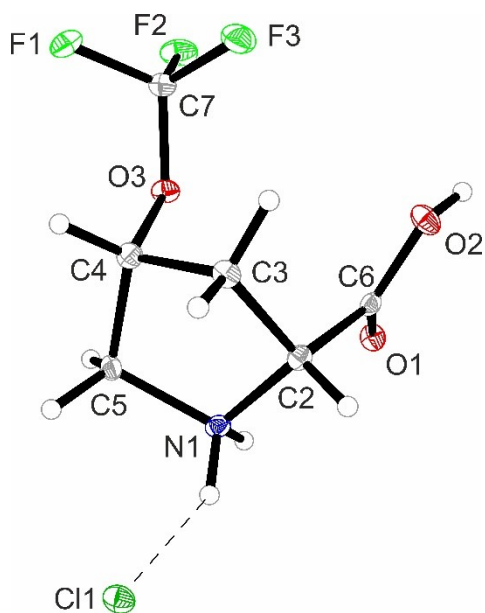


Figure S4. Molecular structure of compound **(2R,4R)-6·HCl** according to X-ray diffraction data. Thermal ellipsoids are shown at 30 % probability.

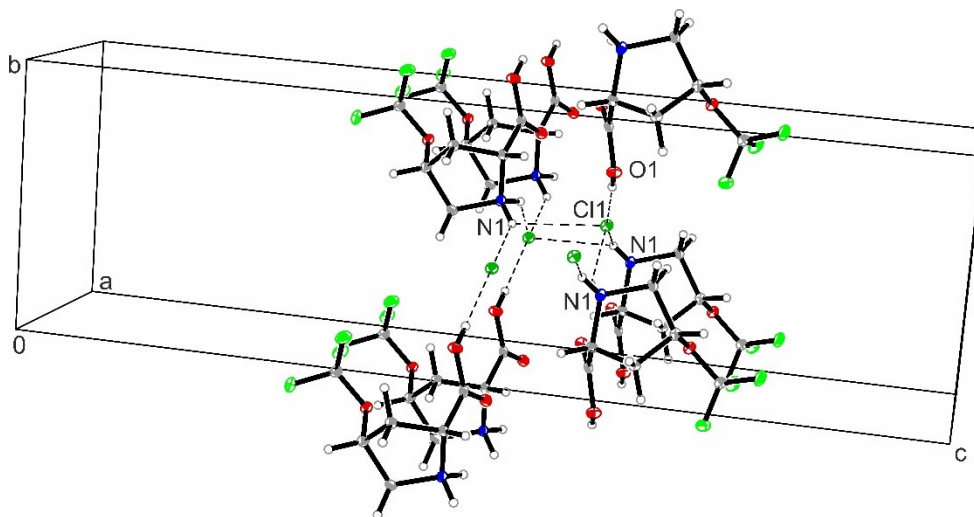


Figure S6. Excerpt of the packing diagram of **(2R,4R)-6·HCl** presenting the formations of N-H...Cl and O-H...Cl hydrogen bonds interactions

The compounds **(2S,4S)-6·HCl**, **(2S,4R)-6·HCl** and **(2R,4S)-6·HCl** exist as hydrochloride salts in the crystal phase (Fig. S1–S3). The heterocycle adopts an envelope conformation where the C3 atom deviates from the plane of the remaining cyclic atoms by $-0.58052(2)$ Å in **(2S,4S)-6·HCl**, $0.618(5)$ Å in **(2S,4R)-6·HCl** and $-0.619(6)$ Å in **(2R,4S)-6·HCl**. The carboxyl group and trifluoromethoxy substituent are located in axial positions (the C5–N1–C2–C6 and N1–C5–C4–O3 torsion angles are $102.8(2)^\circ$ and $-90.9(2)^\circ$, respectively) in the compound **(2S,4S)-6·HCl** (Fig. S1). In the compounds **(2S,4R)-6·HCl** and **(2R,4S)-6·HCl**, the carboxyl group is located in an equatorial position (the C5–N1–C2–C6 torsion angle is $143.8(3)^\circ$ in **(2S,4R)-6·HCl** and $-143.5(3)^\circ$ in **(2R,4S)-6·HCl**) while the trifluoromethoxy substituent is found in an axial position (the N1–C5–C4–O3 torsion angle is $84.9(3)^\circ$ in **(2S,4R)-6·HCl** and $-84.5(4)^\circ$ in **(2R,4S)-6·HCl**).

Molecules of **(2S,4S)-6·HCl**, **(2S,4R)-6·HCl** and **(2R,4S)-6·HCl** are bound with chloride anion by O–H/N–H...Cl intermolecular hydrogen bonds (Table S1) forming double layers parallel to the (001) crystallographic plane in the crystals of **(2S,4S)-6·HCl** or 3D-hydrogen bonded structure in the crystals of **(2S,4R)-6·HCl** and **(2R,4S)-6·HCl** (Fig. S4).

X-Ray analysis of compounds **(2R,4R)-6·HCl** was performed on other instrument. According to the data geometric characteristics are similar to **(2S,4S)-6·HCl** (Fig. S5, S6 and Table 2)

Table S1. Intermolecular hydrogen bonds and their geometric characteristics in crystals of **(2S,4S)-6·HCl**, **(2S,4R)-6·HCl** and **(2R,4S)-6·HCl**.

Hydrogen bond	Symmetry operation	Geometric characteristics		
		H...A, Å	D...Å, Å	D–H...A, deg
Structure (2S,4S)-6·HCl				
N1–H...Cl1'	x,y,z	2.42	3.192(2)	142.7
N1–H...Cl1'	$x-1,y,z$	2.33	3.108(2)	143.6
O2–H...Cl1'	$x,y-1,z$	2.14	2.964(2)	168.9
Structure (2S,4R)-6·HCl				
N1–H...Cl1'	x,y,z	2.20	3.042(3)	152.9

N1–H...Cl1'	0.5+x,1.5-y,1-z	2.37	3.210(3)	152.6
O2–H...Cl1'	1.5-x,2-y,0.5+z	2.14	2.981(3)	174.0
Structure (2R,4S)-6·HCl				
N1–H...Cl1'	x,y,z	2.20	3.036(3)	152.9
N1–H...Cl1'	0.5+x,1.5-y,1-z	2.37	3.200(3)	152.3
O2–H...Cl1'	1.5-x,2-y,-0.5+z	2.14	2.981(4)	174.2

Table S2. Hydrogen bond interactions in compound **(2R,4R)-6·HCl** (Å and deg)^a

D-H...A	d(D-H)	d(H...A)	d(D...A)	∠(DHA)
N1-H1A...Cl1 ^{#1}	0.95(4)	2.39(4)	3.176(4)	141(3)
N1-H1B...Cl1	0.90(4)	2.36(4)	3.102(3)	140(3)
O2-H2A...Cl1 ^{#2}	0.82(5)	2.15(5)	2.966(5)	178(4)

Symmetry transformations used to generate equivalent atoms: ^{#1} x+1, y, z; ^{#2} x+1, y+1, z.

X-Ray diffraction: For compound **(2S,4R)-6·HCl**, **(2S,4S)-6·HCl**, **(2R,4S)-6·HCl**, data sets were collected with a Bruker APEX II diffractometer (graphite monochromated MoK α radiation, CCD detector, ϕ - and ω -scanning, $2\theta_{\max} = 50^\circ$). The structure was solved by direct method using *SHELXT-2015* (Sheldrick, G. M. *Acta Cryst.*, **2015**, *A71*, 3-8); structure refinement was done by *SHELXL-2015* (Sheldrick, G. M. *Acta Cryst.*, **2015**, *C71* (1), 3-8).

X-ray crystal structure analysis of (2S,4S)-6·HCl. The colorless crystals of compound **(2S,4S)-6·HCl** (C₆H₉F₃NO₃Cl) are orthorhombic. At 173 K $a = 5.4474(2)$, $b = 7.0132(3)$, $c = 23.9996(11)$ Å, $V = 916.87(7)$ Å³, $M_r = 235.59$, $Z = 4$, space group $P2_12_12_1$, $d_{\text{calc}} = 1.707$ g/cm³, $\mu(\text{MoK}\alpha) = 0.447$ mm⁻¹, $F(000) = 480$. Intensities of 12961 reflections (1625 independent, $R_{\text{int}} = 0.034$) were collected. The absorption correction was performed using the 'multi-scan' method ($T_{\min} = 0.916$, $T_{\max} = 0.961$). The configuration of the asymmetric centres was confirmed by the Flack parameter (0.00(3)). Positions of the hydrogen atoms were located from electron density difference maps and refined using "riding" model with $U_{\text{iso}} = nU_{\text{eq}}$ ($n = 1.5$ for hydroxyl group and $n = 1.2$ for other hydrogen atoms) of the carrier atom. Full-matrix least-squares refinement against F^2 in anisotropic approximation for non-hydrogen atoms using 1625 reflections was converged to $wR_2 = 0.0645$ ($R_1 = 0.0277$ for 1557 reflections with $F > 4\sigma(F)$, $S = 1.092$). CCDC number 2358277.

X-ray crystal structure analysis of (2S,4R)-6·HCl. The colorless crystals of compound **(2S,4R)-6·HCl** (C₆H₉F₃NO₃Cl) are orthorhombic. At 173 K $a = 8.3231(7)$, $b = 8.6507(7)$, $c = 13.3347(11)$ Å, $V = 960.11(14)$ Å³, $M_r = 235.59$, $Z = 4$, space group $P2_12_12_1$, $d_{\text{calc}} = 1.630$ g/cm³, $\mu(\text{MoK}\alpha) = 0.427$ mm⁻¹, $F(000) = 480$. Intensities of 6951 reflections (1691 independent, $R_{\text{int}} = 0.0332$) were collected. The absorption correction was performed using the 'multi-scan' method ($T_{\min} = 0.920$, $T_{\max} = 0.967$). The configuration of the asymmetric centres was confirmed by the Flack parameter (-0.12(4)). Positions of the hydrogen atoms were located from electron density difference maps and refined using "riding" model with $U_{\text{iso}} = nU_{\text{eq}}$ ($n = 1.5$ for hydroxyl group and $n = 1.2$ for other hydrogen atoms) of the carrier atom. Full-matrix least-squares refinement against F^2 in anisotropic approximation for non-hydrogen atoms using 1691 reflections was converged to $wR_2 = 0.073$ ($R_1 = 0.0316$ for 1518 reflections with $F > 4\sigma(F)$, $S = 1.080$). CCDC number 2358276.

X-ray crystal structure analysis of (2R,4S)-6·HCl. The colorless crystals of compound **(2R,4S)-6·HCl** (C₆H₉F₃NO₃Cl) are orthorhombic. At 173 K $a = 8.3057(10)$, $b = 8.6418(8)$, $c = 13.3140(12)$ Å, $V = 955.63(17)$ Å³, $M_r = 235.59$, $Z = 4$, space group $P2_12_12_1$, $d_{\text{calc}} = 1.637$ g/cm³, $\mu(\text{MoK}\alpha) = 0.429$ mm⁻¹, $F(000) = 480$. Intensities of 6475 reflections (1677 independent, $R_{\text{int}} = 0.0542$) were collected. The absorption correction was performed using the 'multi-scan' method ($T_{\min} = 0.919$, $T_{\max} = 0.975$). The configuration of the asymmetric centres was confirmed by the Flack parameter (-0.06(6)). Positions of the hydrogen atoms were located from electron density difference maps and refined using "riding" model with $U_{\text{iso}} = nU_{\text{eq}}$ ($n = 1.5$ for hydroxyl group and $n = 1.2$ for other hydrogen atoms) of the carrier atom. Full-matrix least-squares refinement against F^2 in anisotropic approximation for non-hydrogen atoms using 1677

reflections was converged to $wR_2 = 0.085$ ($R_1 = 0.0485$ for 1432 reflections with $F > 4\sigma(F)$, $S = 1.131$). CCDC number 2361466

X-Ray diffraction: For compound **(2R,4R)-6·HCl** data sets were collected with a Bruker Kappa CCD APEXII diffractometer. Programs used: data collection: APEX3 V2016.1-0 (Bruker AXS Inc., **2016**); cell refinement: SAINT V8.37A (Bruker AXS Inc., **2015**); data reduction: SAINT V8.37A (Bruker AXS Inc., **2015**); absorption correction, SADABS V2014/7 (Bruker AXS Inc., **2014**); structure solution *SHELXT-2015* (Sheldrick, G. M. *Acta Cryst.*, **2015**, A71, 3-8); structure refinement *SHELXL-2015* (Sheldrick, G. M. *Acta Cryst.*, **2015**, C71 (1), 3-8) and graphics, *XP* (Version 5.1, Bruker AXS Inc., Madison, Wisconsin, USA, **1998**). *R*-values are given for observed reflections, and wR^2 values are given for all reflections.

X-ray crystal structure analysis of (2R,4R)-6·HCl: A colorless needle-like specimen of $C_6H_9ClF_3NO_3$, approximate dimensions 0.020 mm x 0.040 mm x 0.160 mm, was used for the X-ray crystallographic analysis. The X-ray intensity data were measured. A total of 1395 frames were collected. The total exposure time was 23.95 hours. The frames were integrated with the Bruker SAINT software package using a wide-frame algorithm. The integration of the data using an orthorhombic unit cell yielded a total of 7754 reflections to a maximum θ angle of 66.69° (0.84 Å resolution), of which 1612 were independent (average redundancy 4.810, completeness = 99.5%, $R_{int} = 5.59\%$, $R_{sig} = 4.37\%$) and 1461 (90.63%) were greater than $2\sigma(F^2)$. The final cell constants of $a = 5.4353(2)$ Å, $b = 7.0050(3)$ Å, $c = 23.8253(10)$ Å, volume = $907.13(6)$ Å³, are based upon the refinement of the XYZ-centroids of 2122 reflections above $20 \sigma(I)$ with $13.17^\circ < 2\theta < 133.2^\circ$. Data were corrected for absorption effects using the multi-scan method (SADABS). The ratio of minimum to maximum apparent transmission was 0.755. The calculated minimum and maximum transmission coefficients (based on crystal size) are 0.5580 and 0.9220. The structure was solved and refined using the Bruker SHELXTL Software Package, using the space group $P2_12_12_1$, with $Z = 4$ for the formula unit, $C_6H_9ClF_3NO_3$. The final anisotropic full-matrix least-squares refinement on F^2 with 139 variables converged at $R1 = 2.84\%$, for the observed data and $wR2 = 6.62\%$ for all data. The goodness-of-fit was 1.021. The largest peak in the final difference electron density synthesis was $0.269 e^-/\text{Å}^3$ and the largest hole was $-0.188 e^-/\text{Å}^3$ with an RMS deviation of $0.052 e^-/\text{Å}^3$. On the basis of the final model, the calculated density was 1.725 g/cm^3 and $F(000)$, 480 e^- . Flack parameter was refined to 0.04(1). Hydrogen atoms at N1 (H1A and H1B) and O2 (H2A) were refined freely. CCDC number: 2346847.

References:

1. Sheldrick, G. M., *SHELXT – Integrated space-group and crystal-structure determination*, *Acta Cryst.*, **2015**, A71, 3-8.
2. Sheldrick, G.M., *Crystal structure refinement with SHELXL*, *Acta Cryst.*, **2015**, C71 (1), 3-8.
3. *APEX3 (2016)*, *SAINT (2015)* and *SADABS (2015)*, Bruker AXS Inc., Madison, Wisconsin, USA.
- 4.
5. *XP – Interactive molecular graphics, Version 5.1*, Bruker AXS Inc., Madison, Wisconsin, USA, **1998**.
- 6.

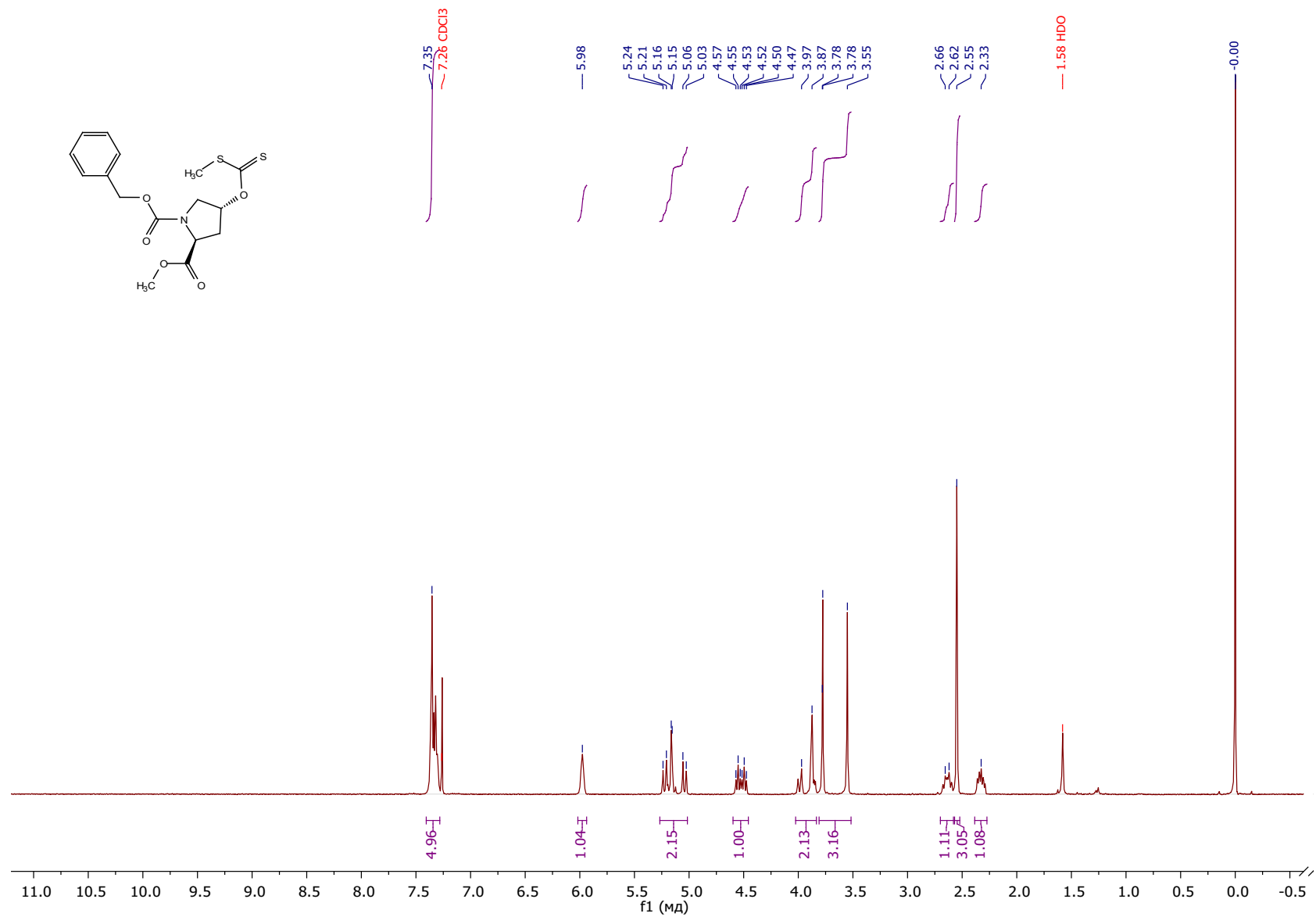


Figure S1. ¹H NMR of Compound (2S,4R)-9 (400 MHz, CDCl₃)

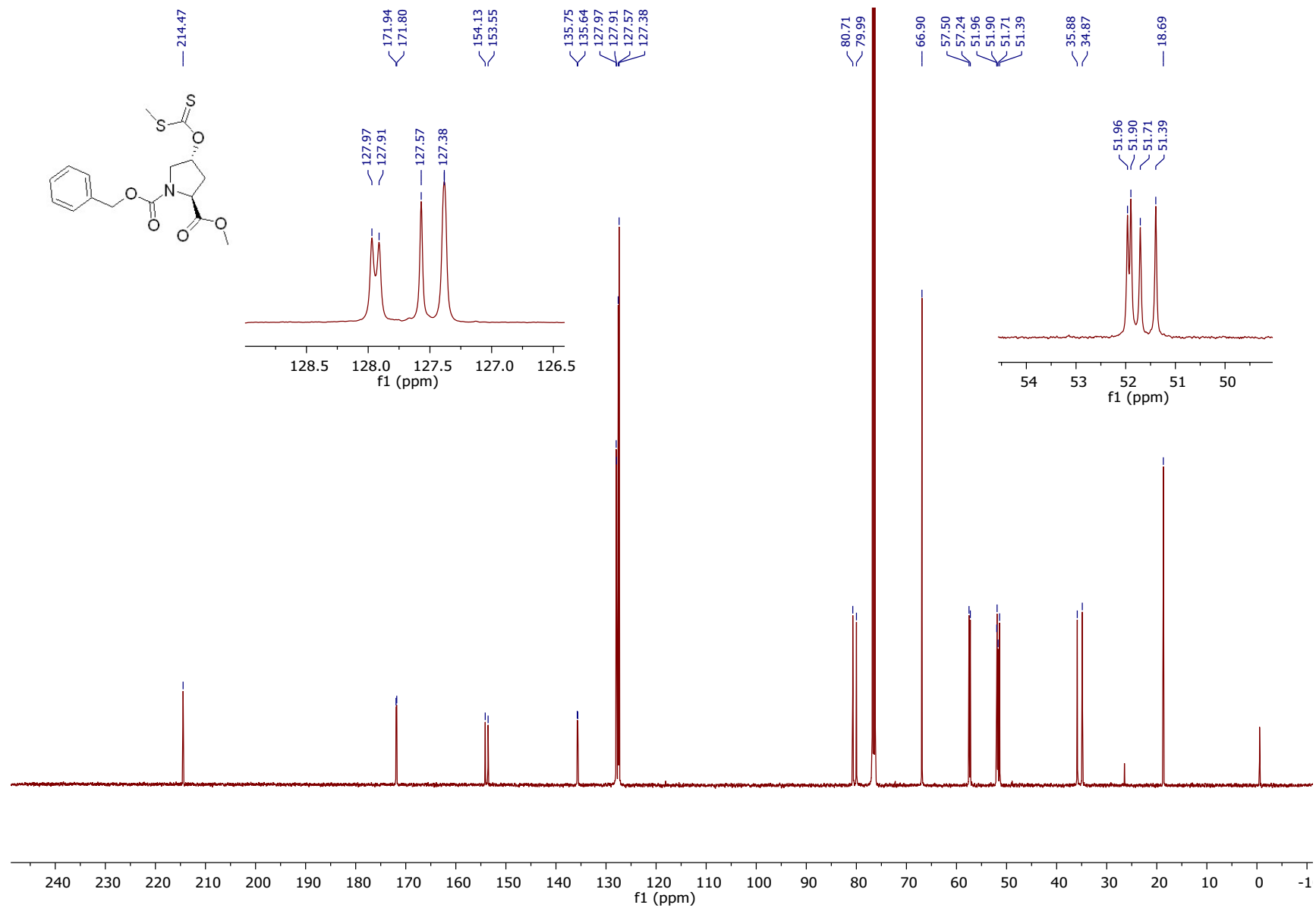


Figure S2. $^{13}\text{C}\{^1\text{H}\}$ NMR of Compound (2S,4R)-9 (151 MHz, CDCl_3)

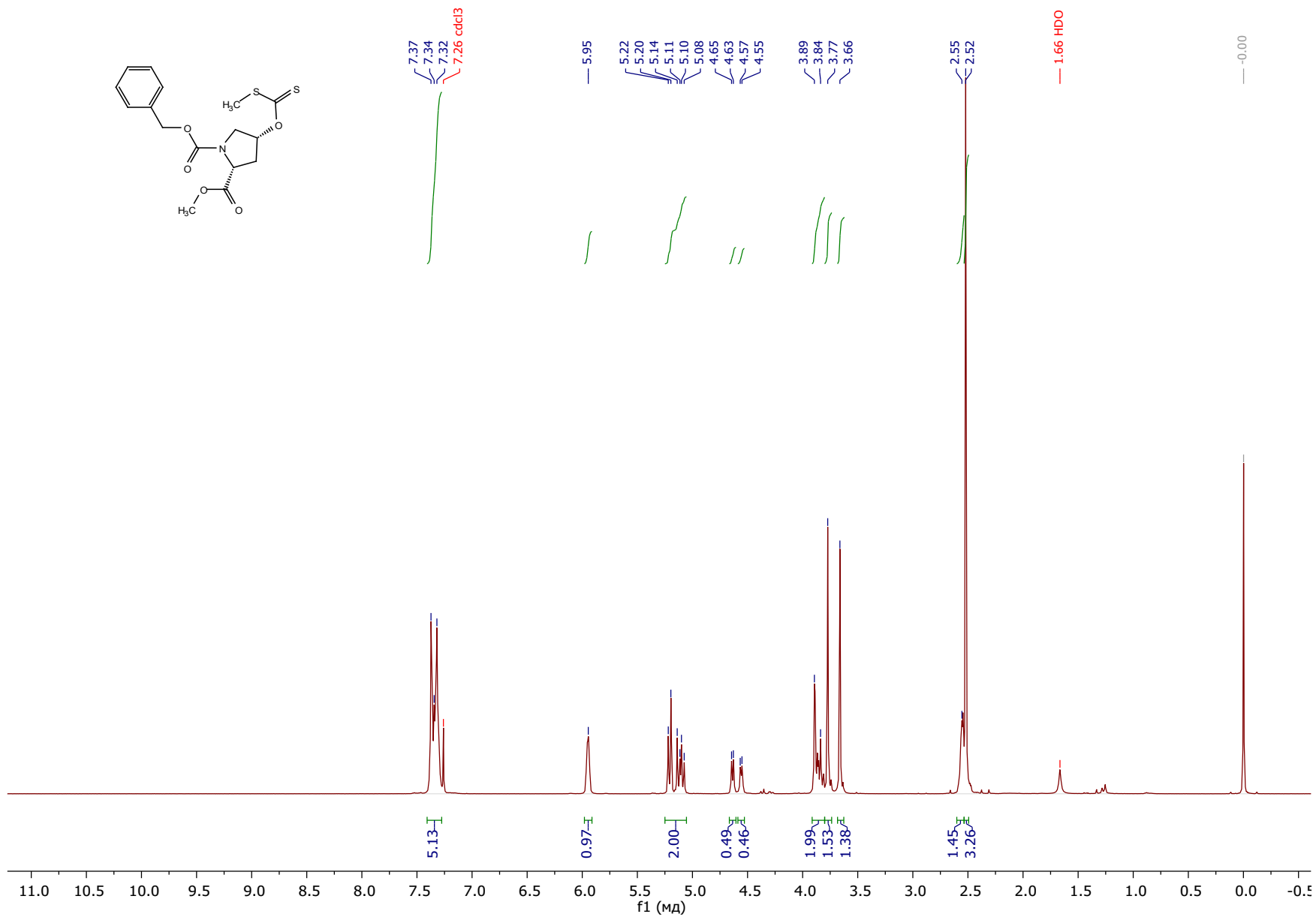


Figure S3. ¹H NMR of Compound (2S,4S)-9 (500 MHz, CDCl₃)

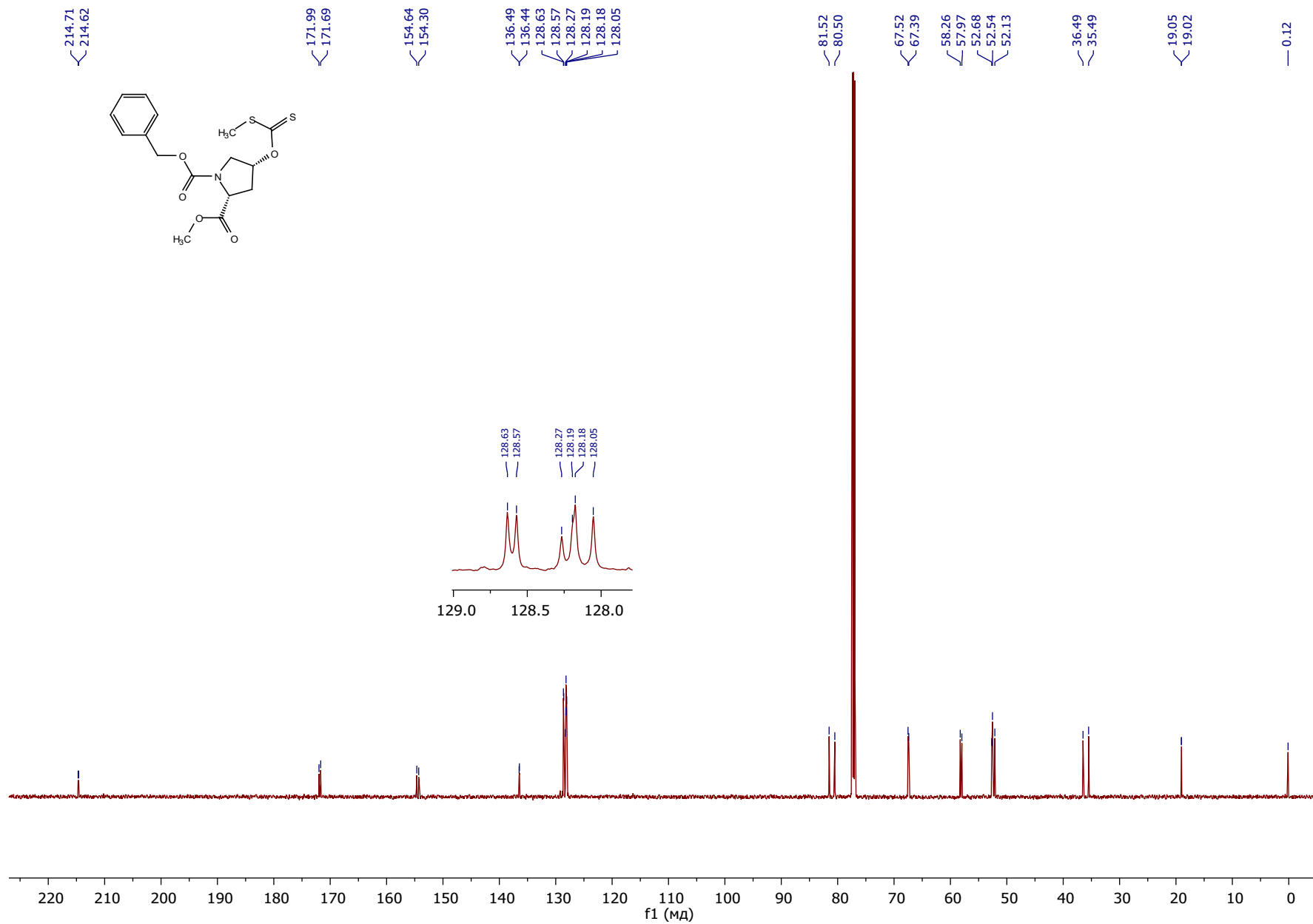


Figure S4. $^{13}\text{C}\{^1\text{H}\}$ NMR of Compound (2S,4S)-9 (151 MHz, CDCl_3)

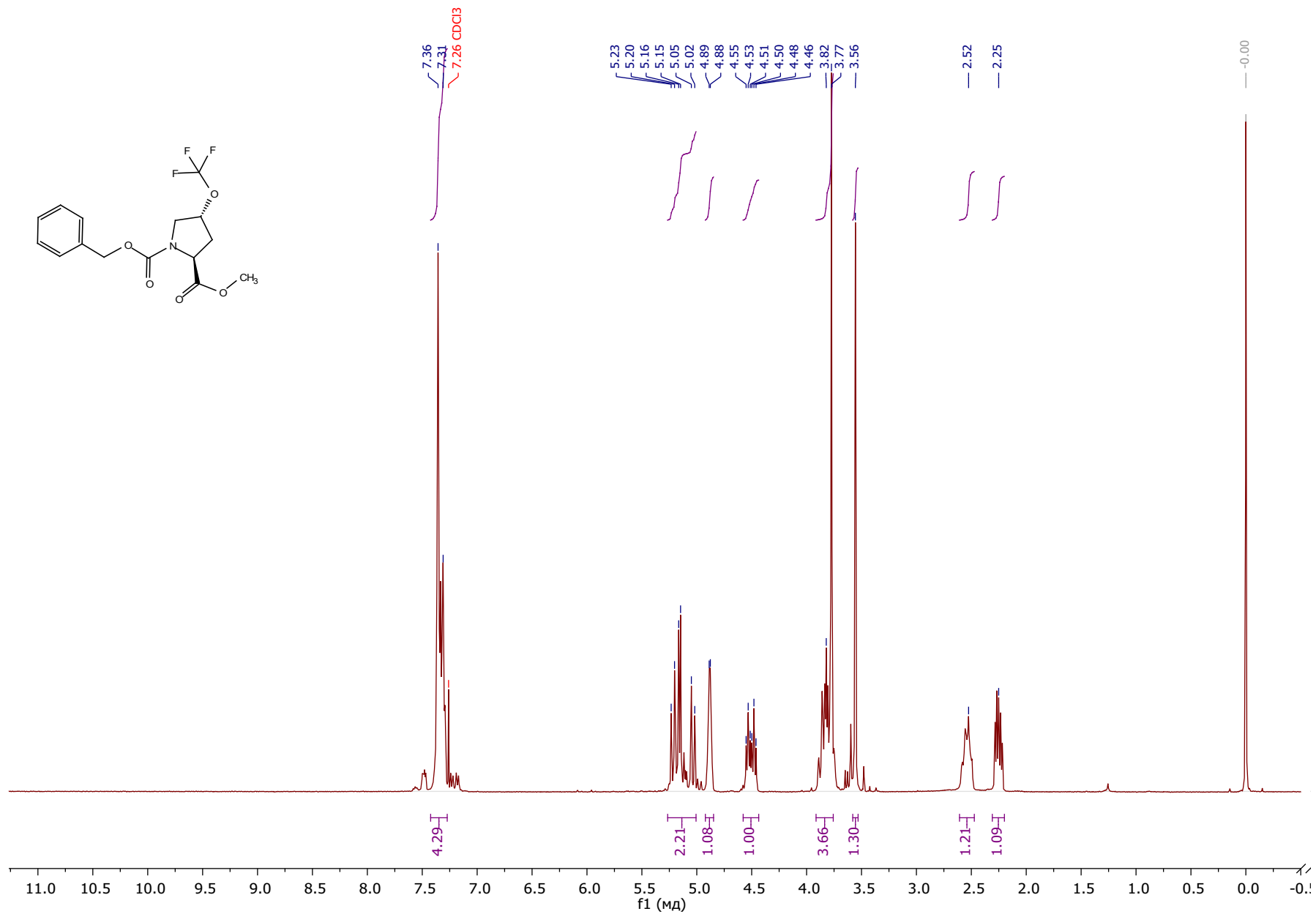


Figure S5. ¹H NMR of Compound (2S,4R)-10 (400 MHz, CDCl₃)

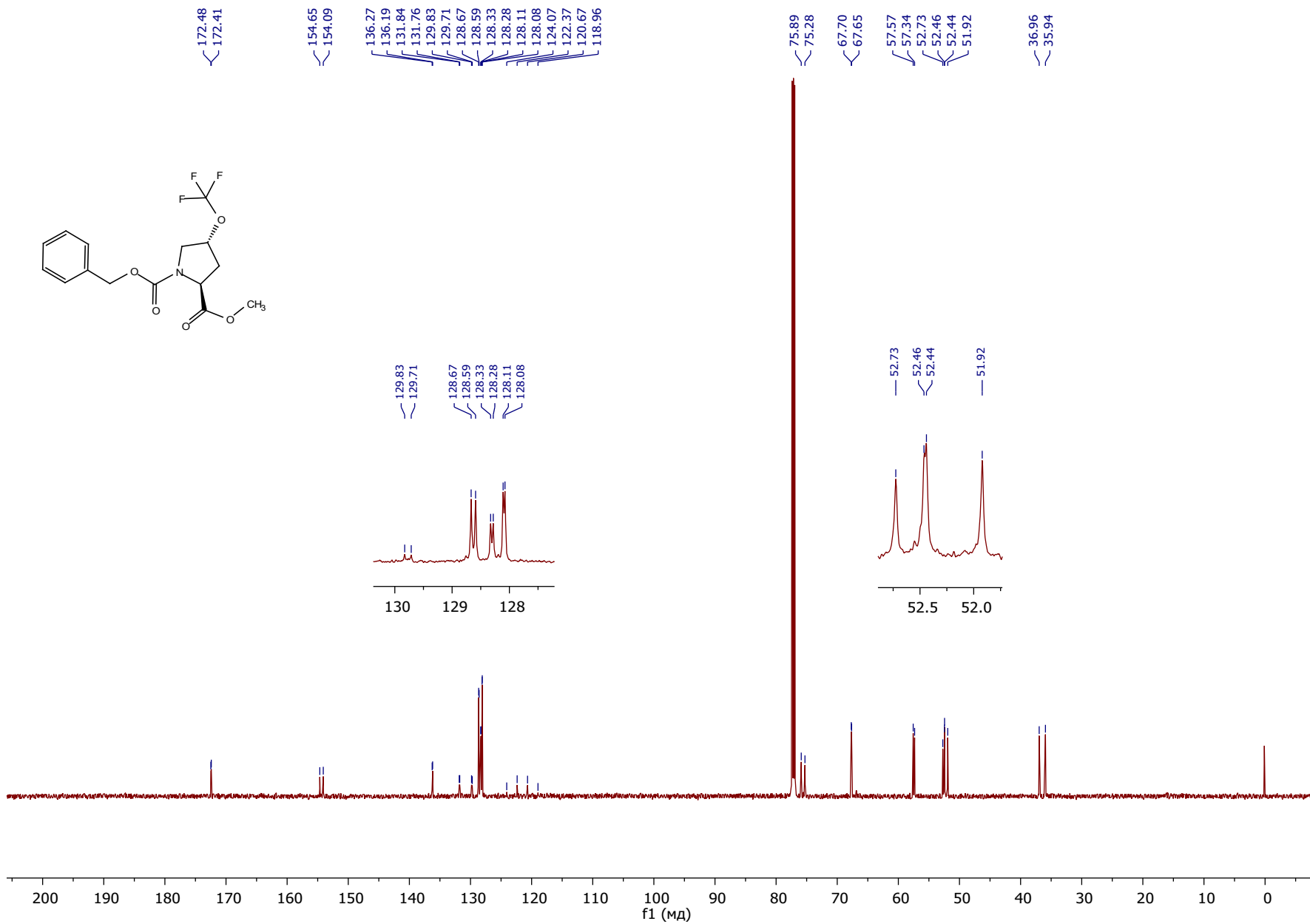


Figure S6. $^{13}\text{C}\{^1\text{H}\}$ NMR of Compound (2S,4R)-10 (151 MHz, CDCl_3)

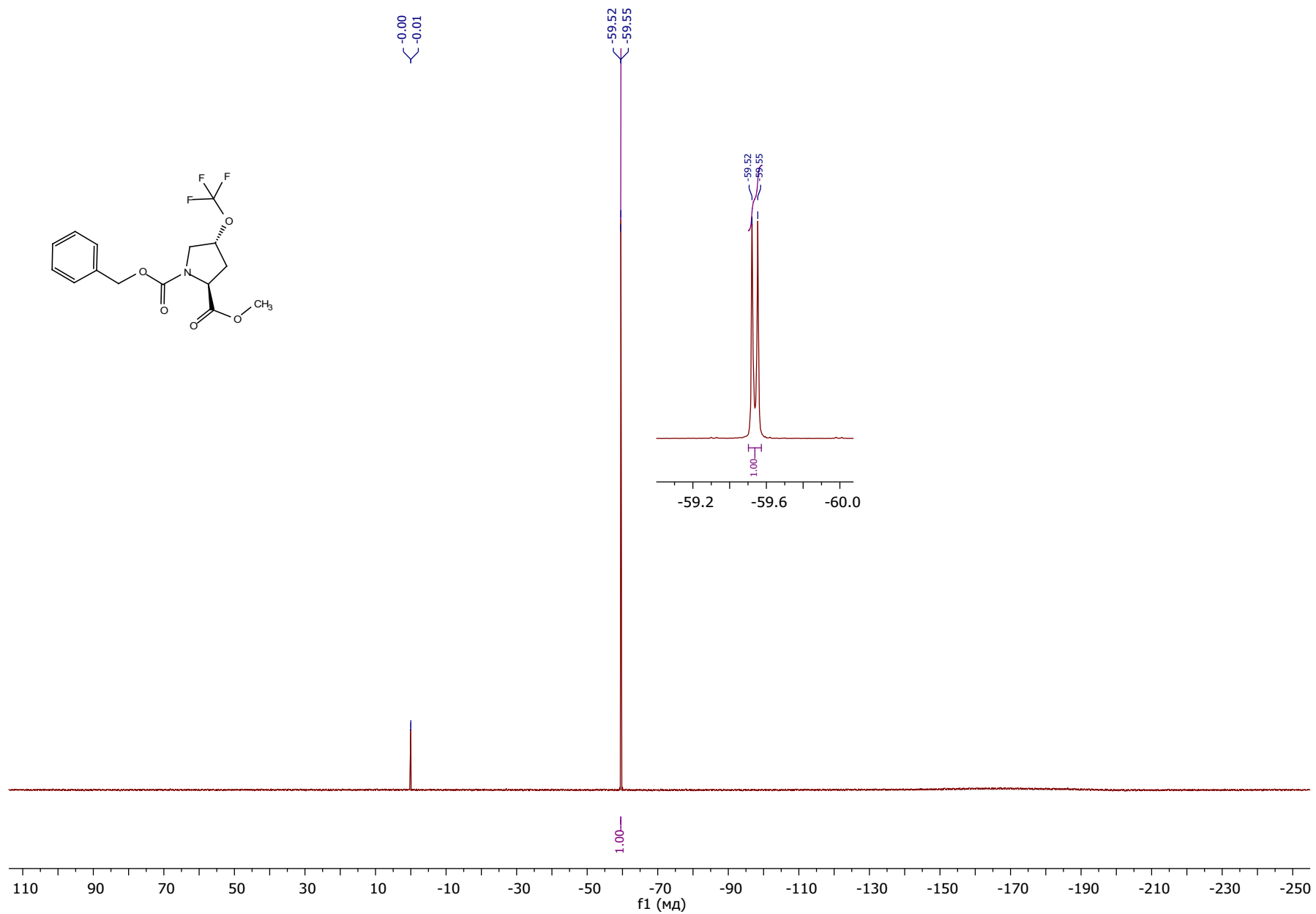


Figure S7. $^{19}\text{F}\{^1\text{H}\}$ NMR of Compound **(2S,4R)-10** (376 MHz, CDCl_3)

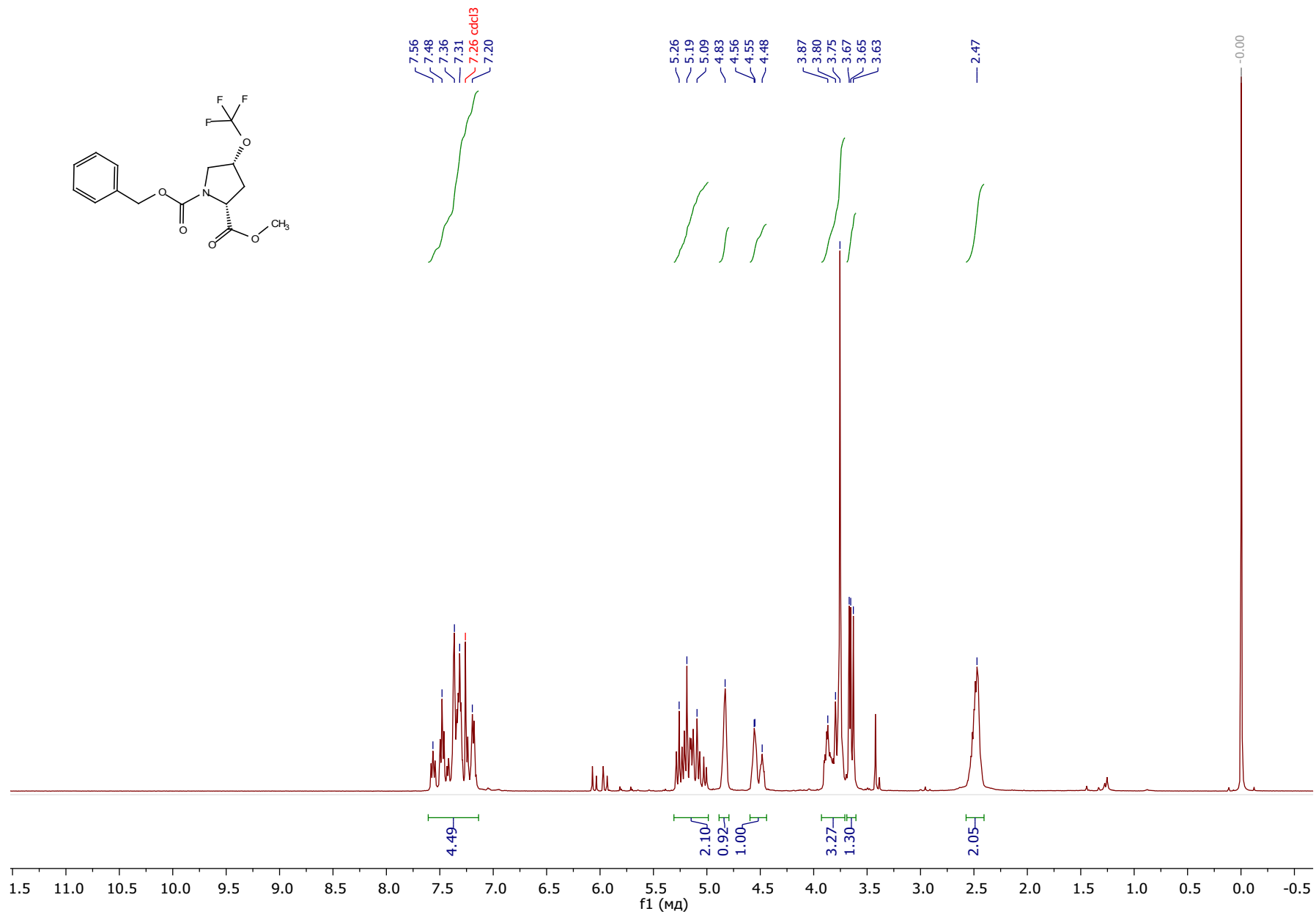


Figure S8. ¹H NMR of Compound (2S,4S)-10 (400 MHz, CDCl₃)

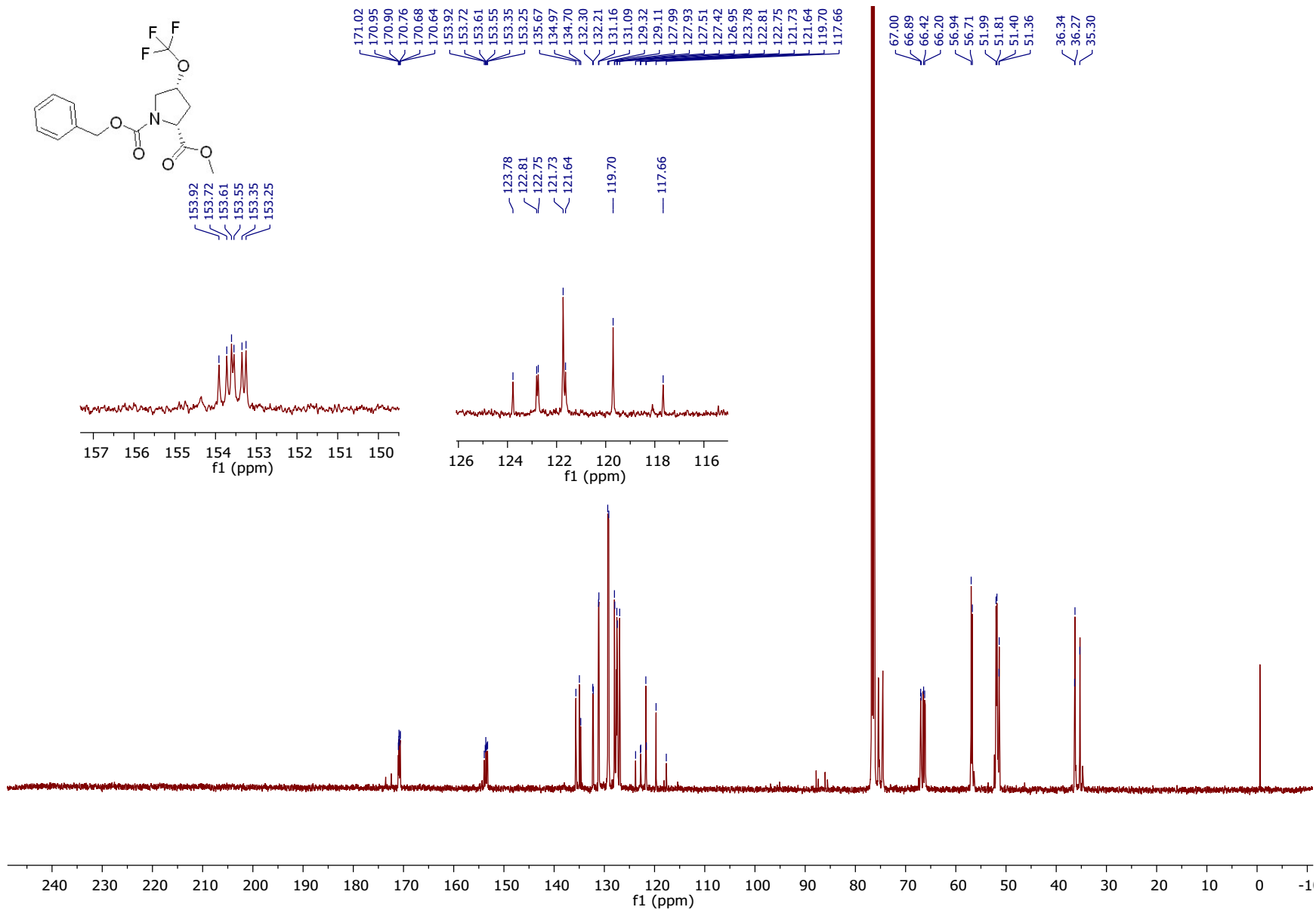


Figure S9. ¹³C{¹H} NMR of Compound (2S,4S)-10 (151 MHz, CDCl₃)

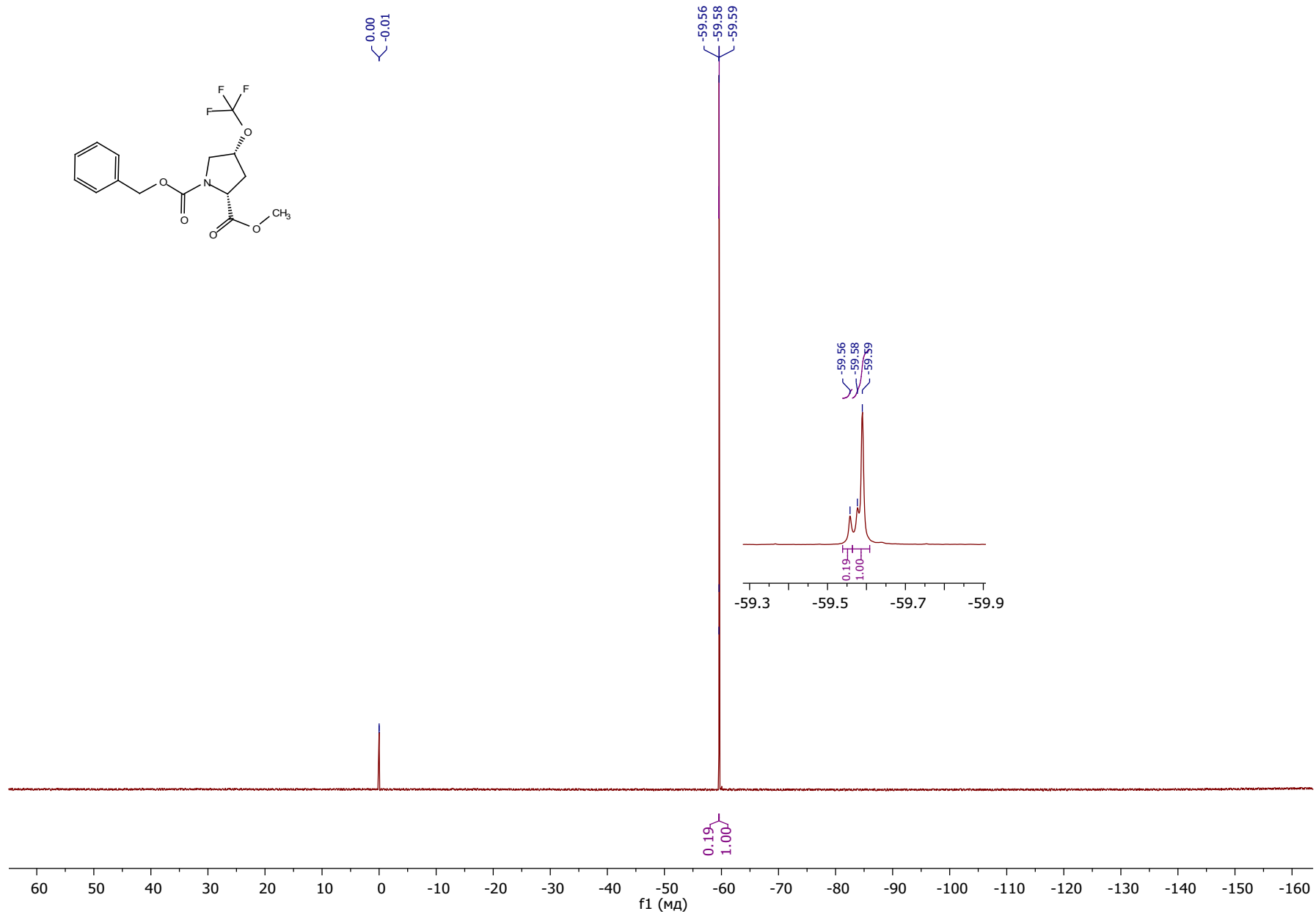


Figure S10. $^{19}\text{F}\{^1\text{H}\}$ NMR of Compound (2S,4S)-10 (376 MHz, CDCl_3)

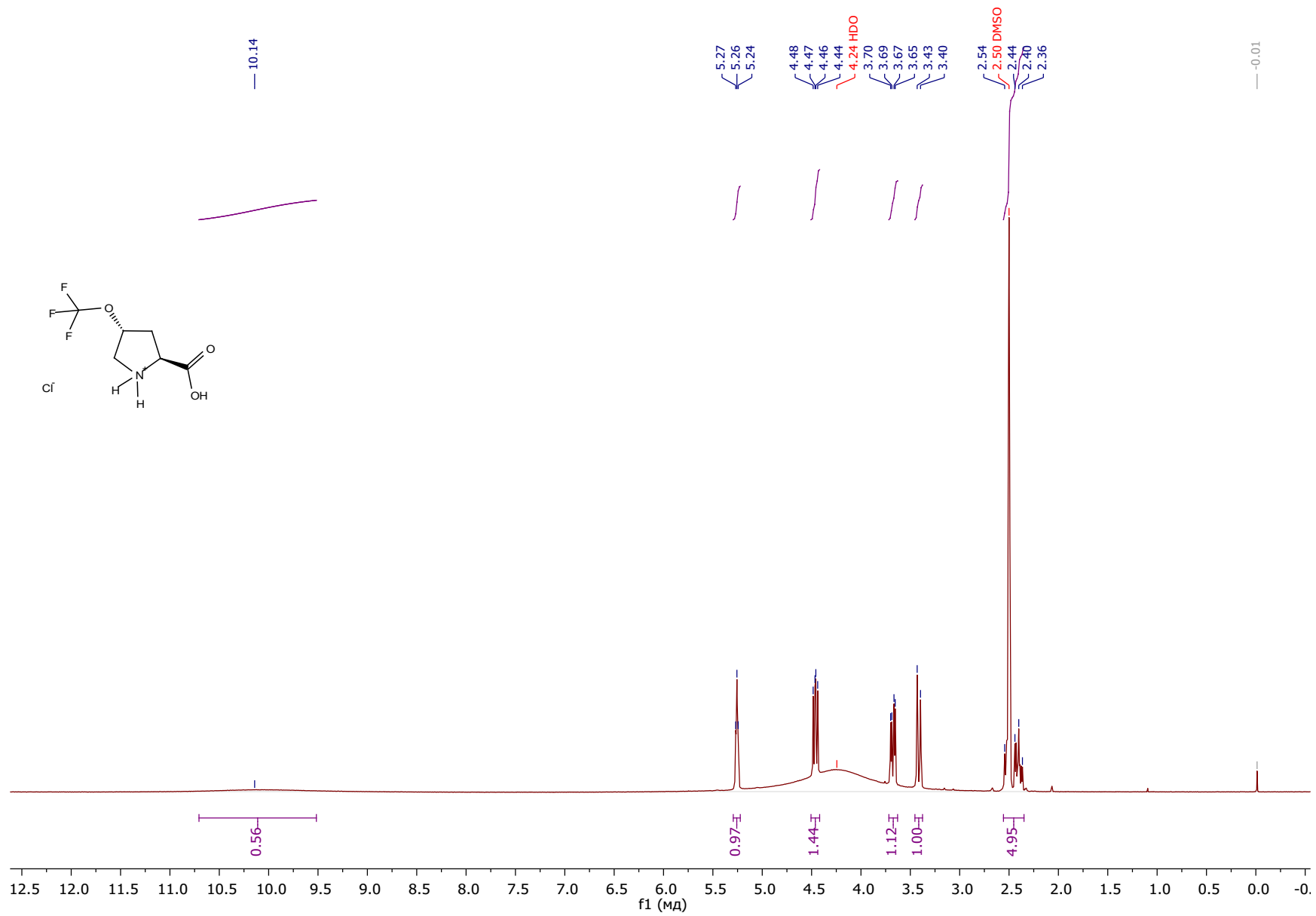


Figure S11. ^1H NMR of Compound (2S,4R)-6-HCl (400 MHz, $\text{DMSO-}d_6$)

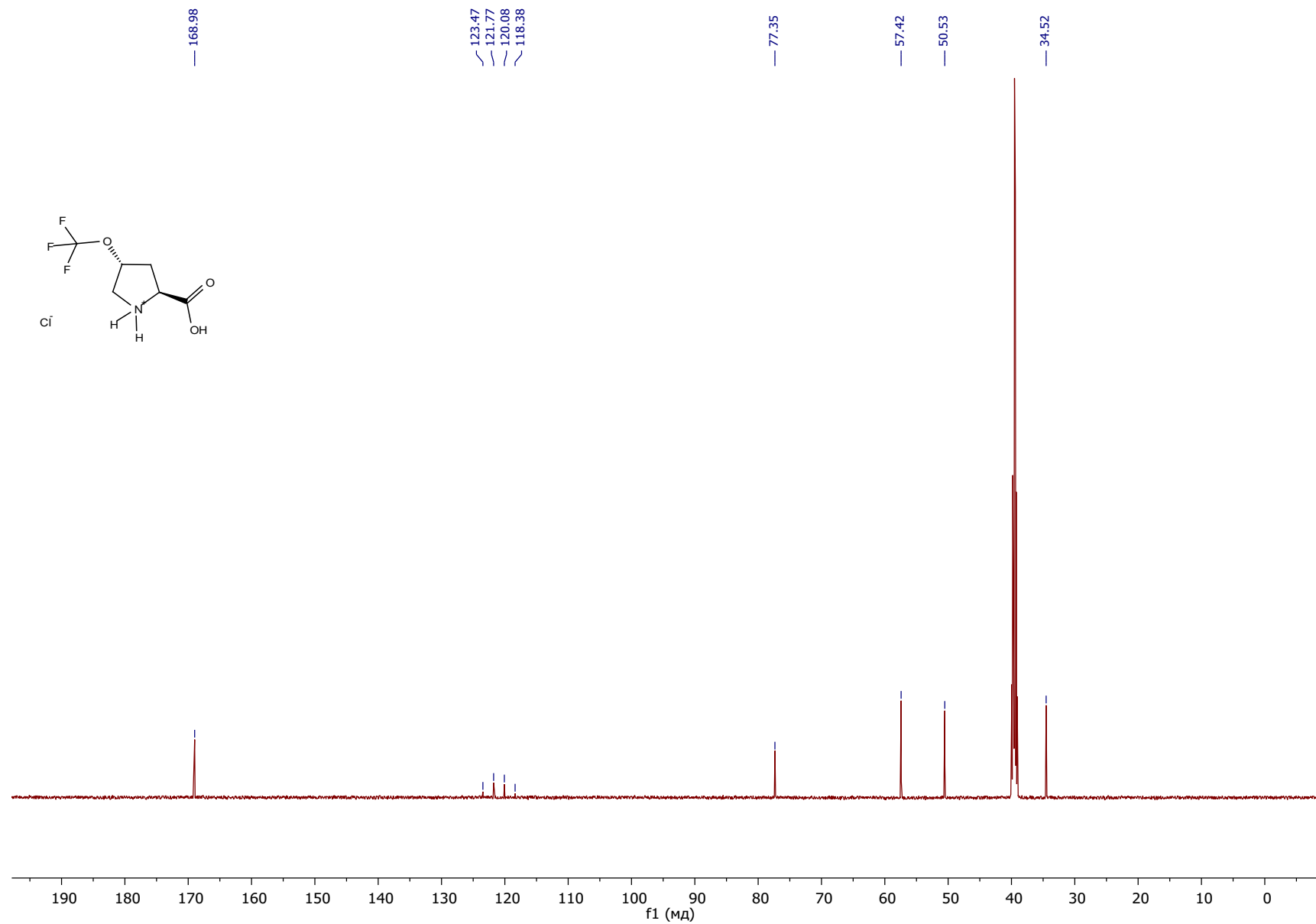


Figure S12. $^{13}\text{C}\{^1\text{H}\}$ NMR of Compound **(2S,4R)-6-HCl** (151 MHz, $\text{DMSO-}d_6$)

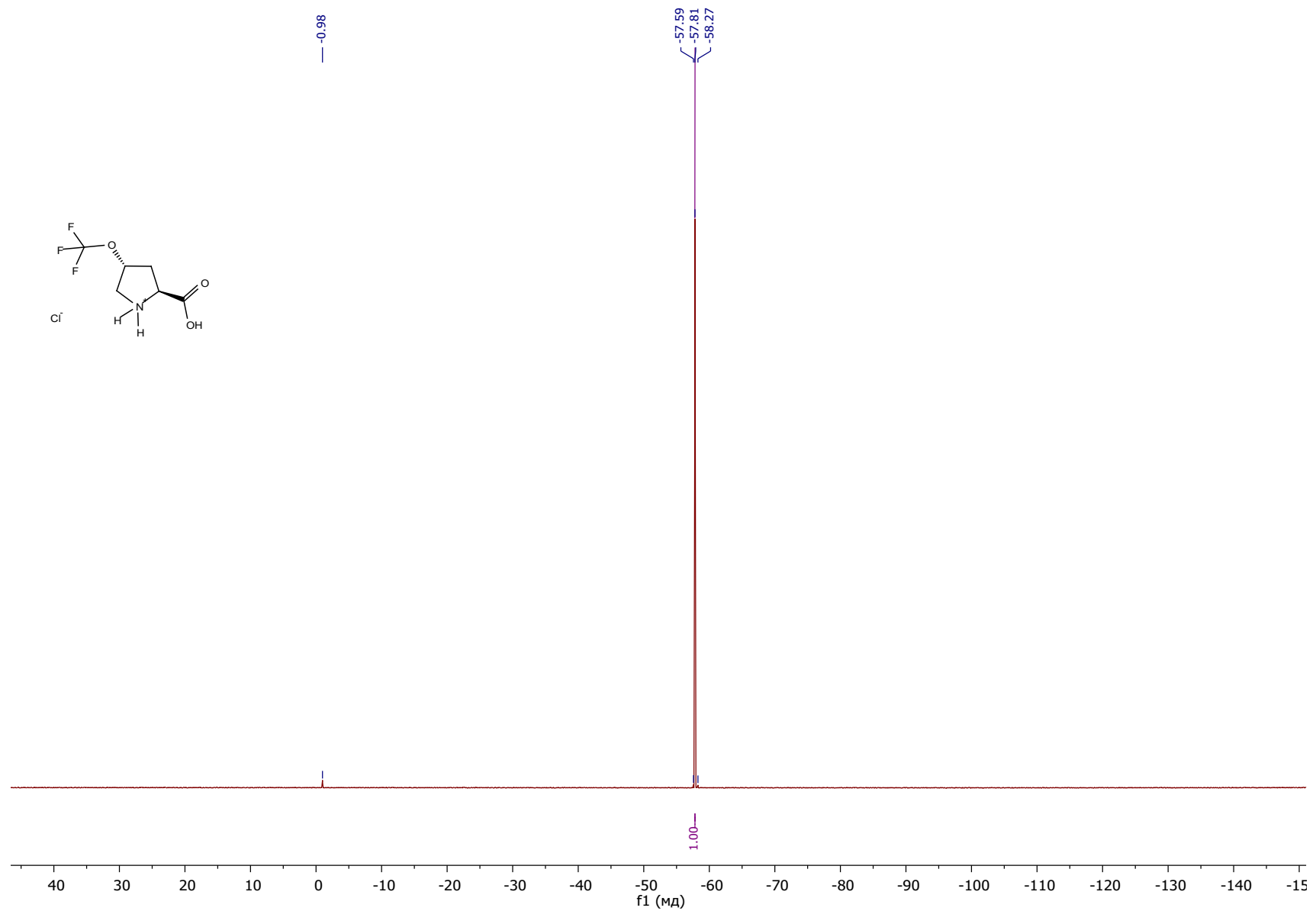


Figure S13. $^{19}\text{F}\{^1\text{H}\}$ NMR of Compound **(2S,4R)-6·HCl** (376 MHz, $\text{DMSO-}d_6$)

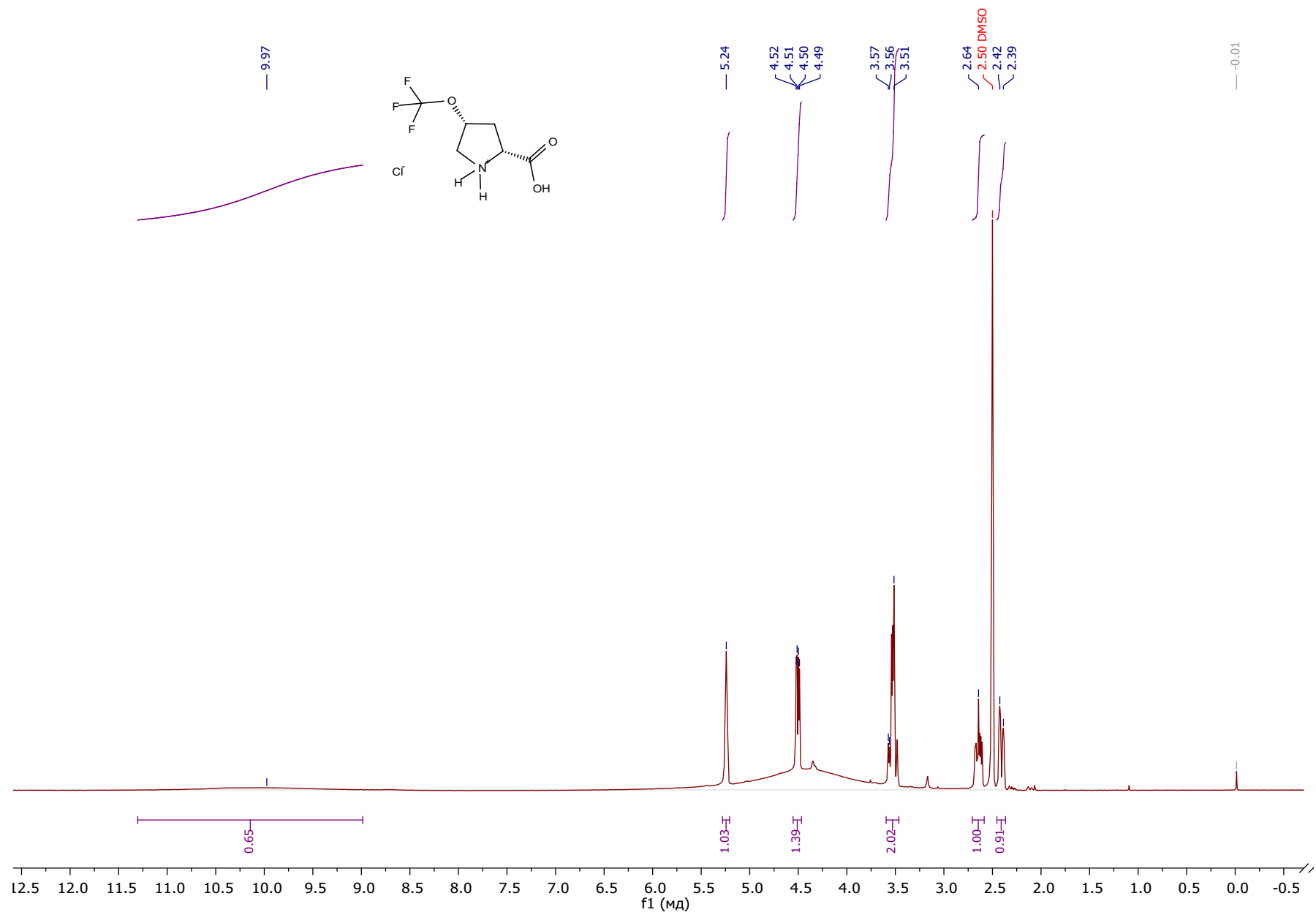


Figure S14. ¹H NMR of Compound (2S,4S)-6·HCl (400 MHz, DMSO-d₆)

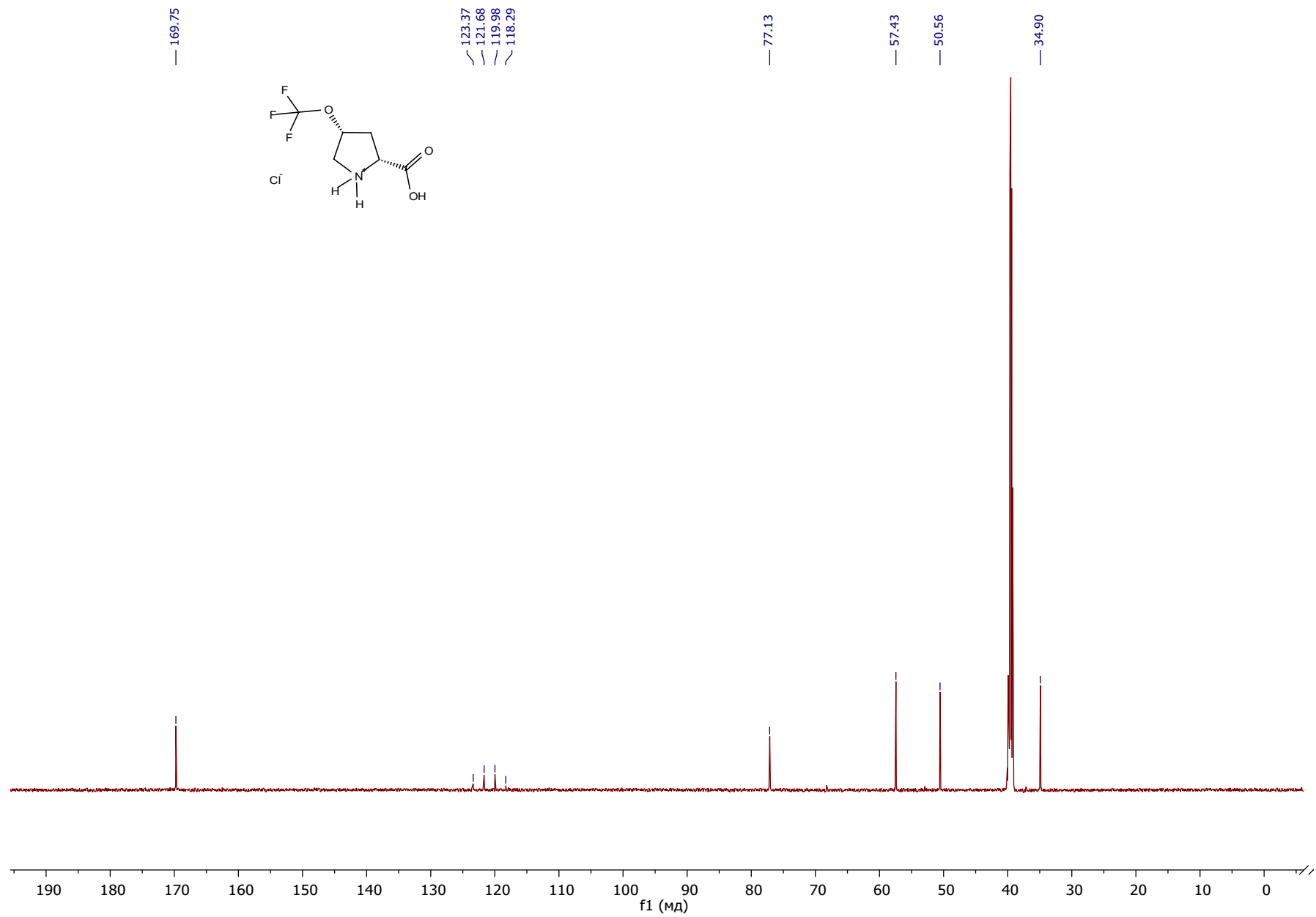


Figure S15. $^{13}\text{C}\{^1\text{H}\}$ NMR of Compound (2S,4S)-6·HCl (151 MHz, DMSO- d_6)

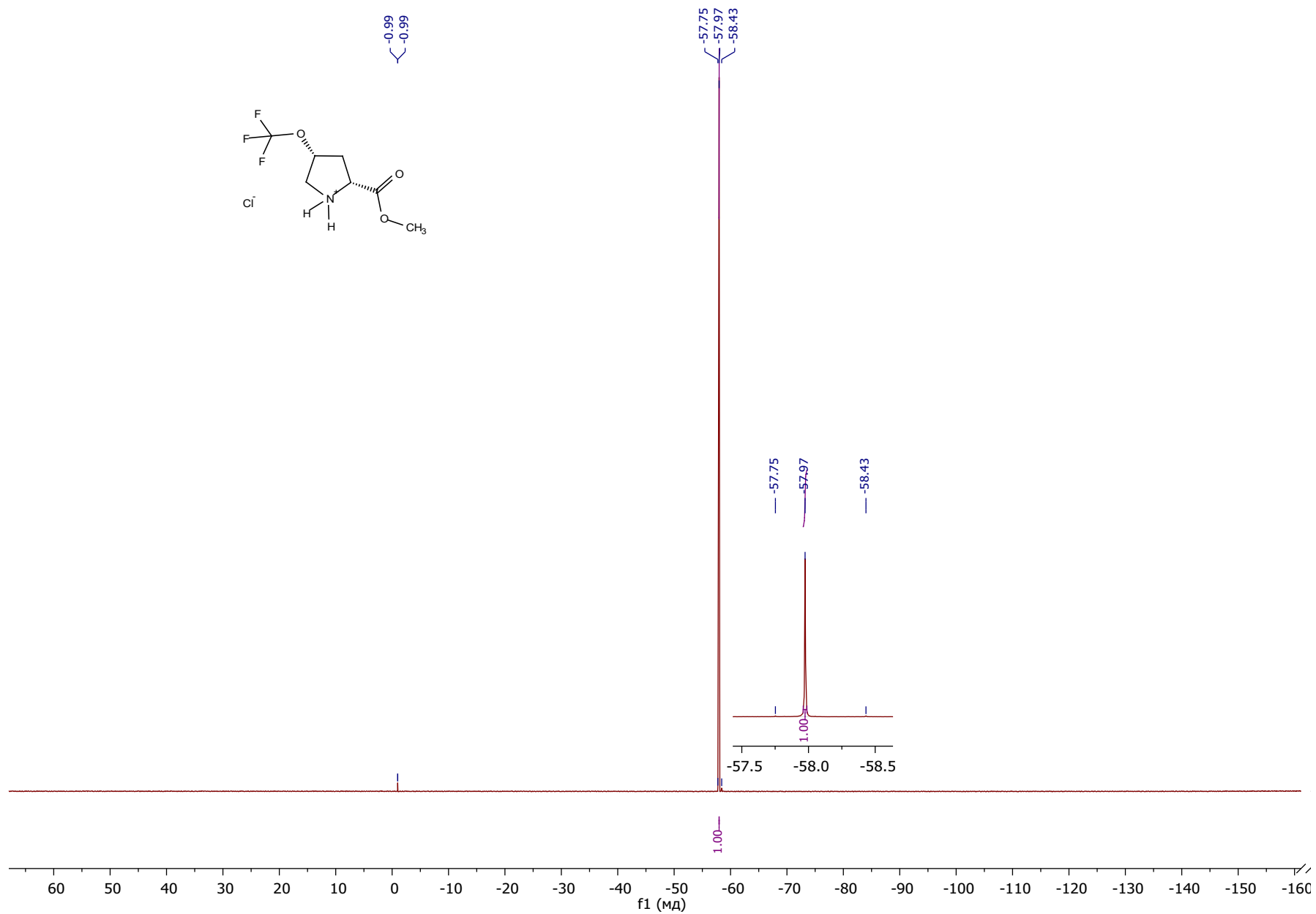


Figure S16. $^{19}\text{F}\{^1\text{H}\}$ NMR of Compound (2S,4S)-6·HCl (376 MHz, DMSO- d_6)

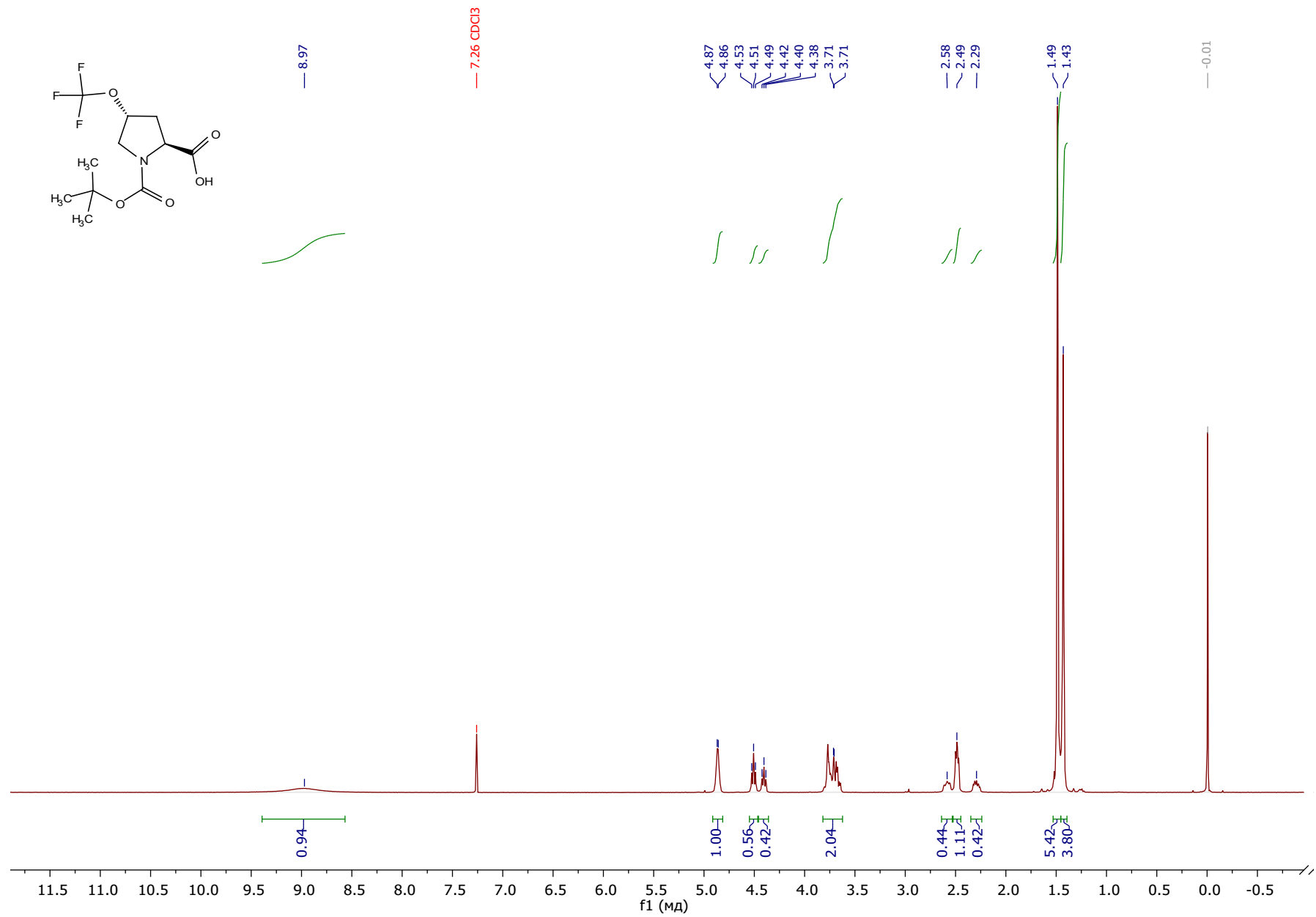


Figure S17. ¹H NMR of Compound (2S,4R)-11 (400 MHz, CDCl₃)

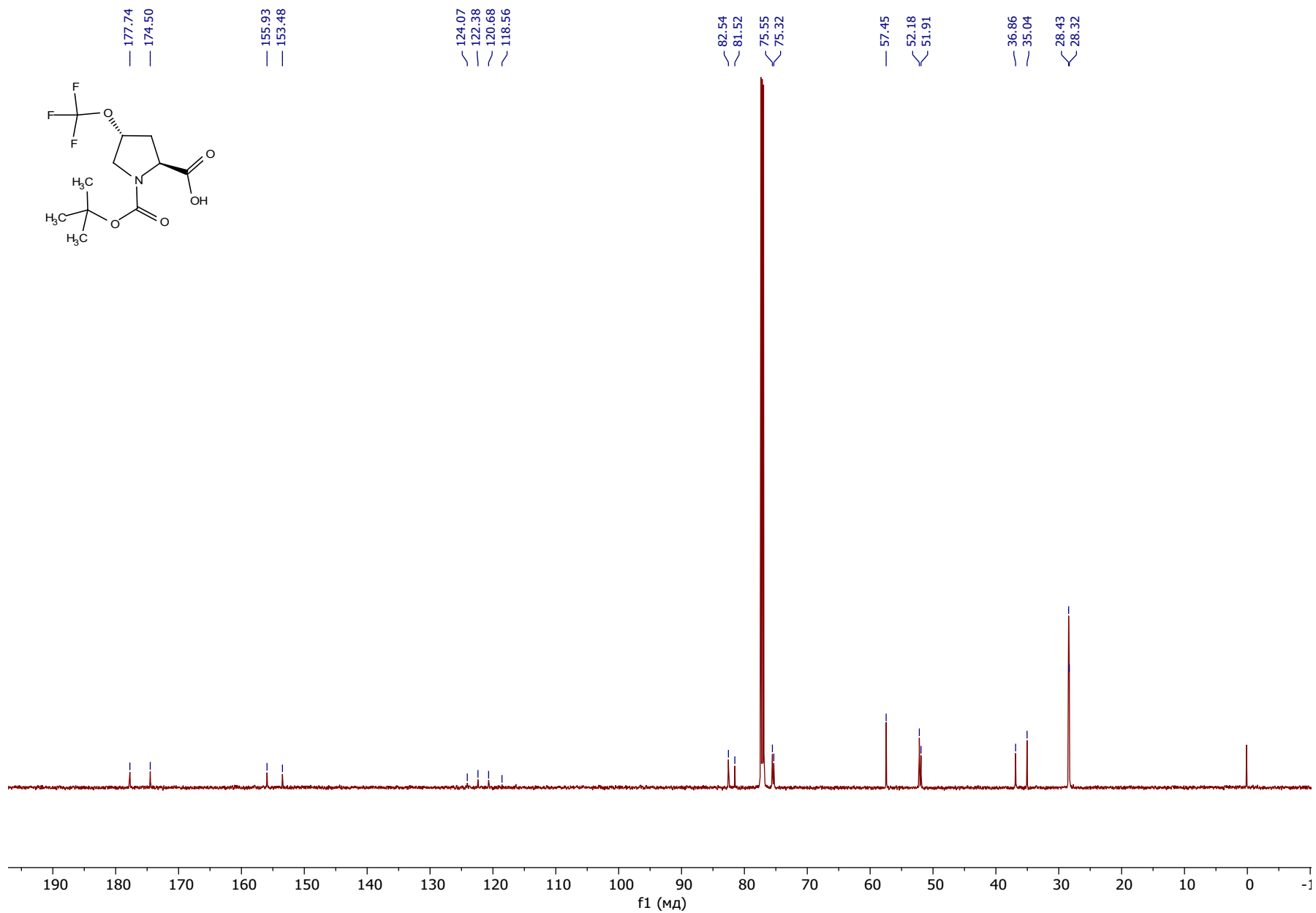
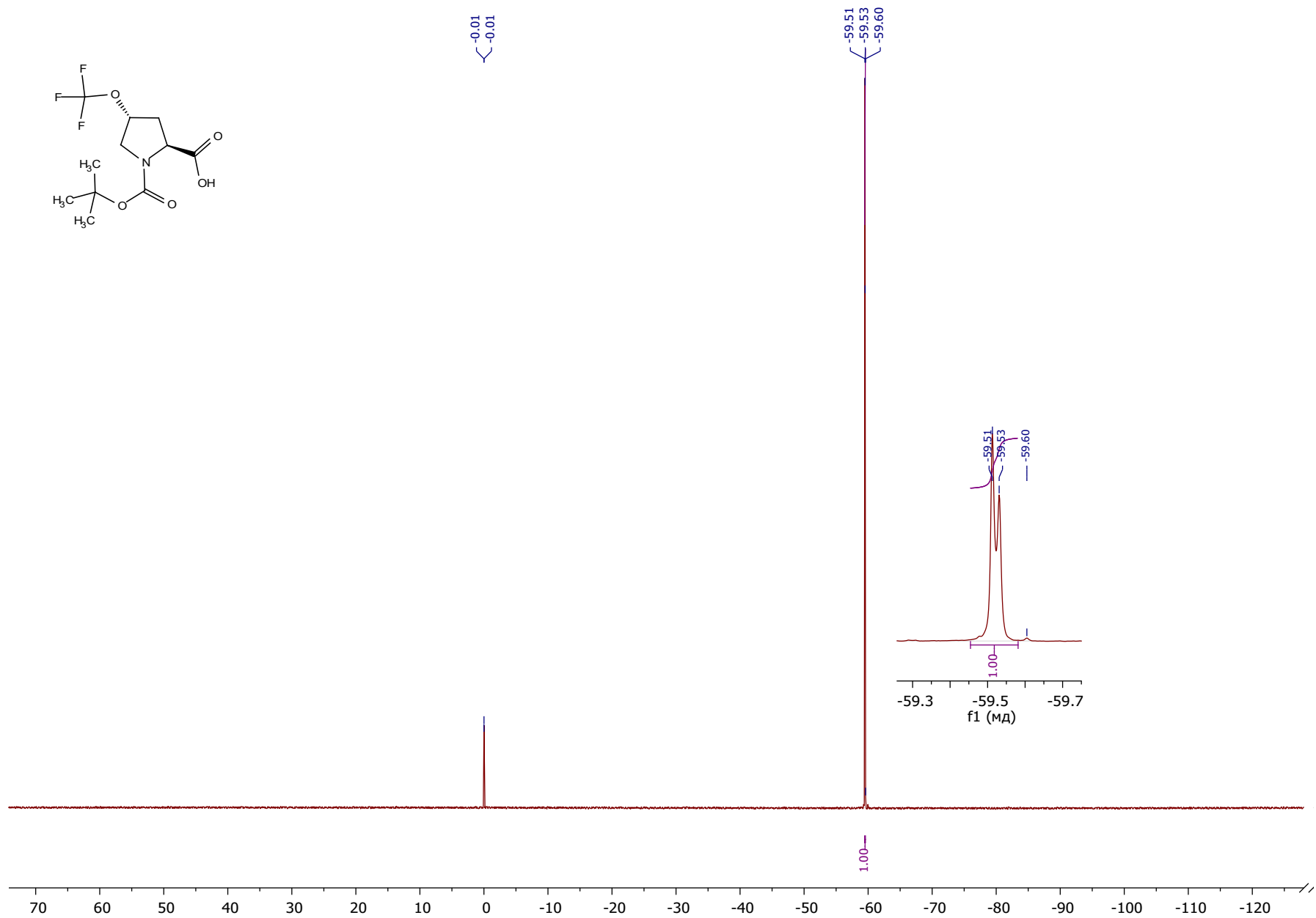
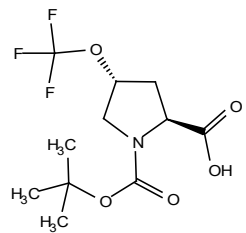


Figure S18. ¹³C{¹H} NMR of Compound **(2S,4R)-11** (151 MHz, CDCl₃)



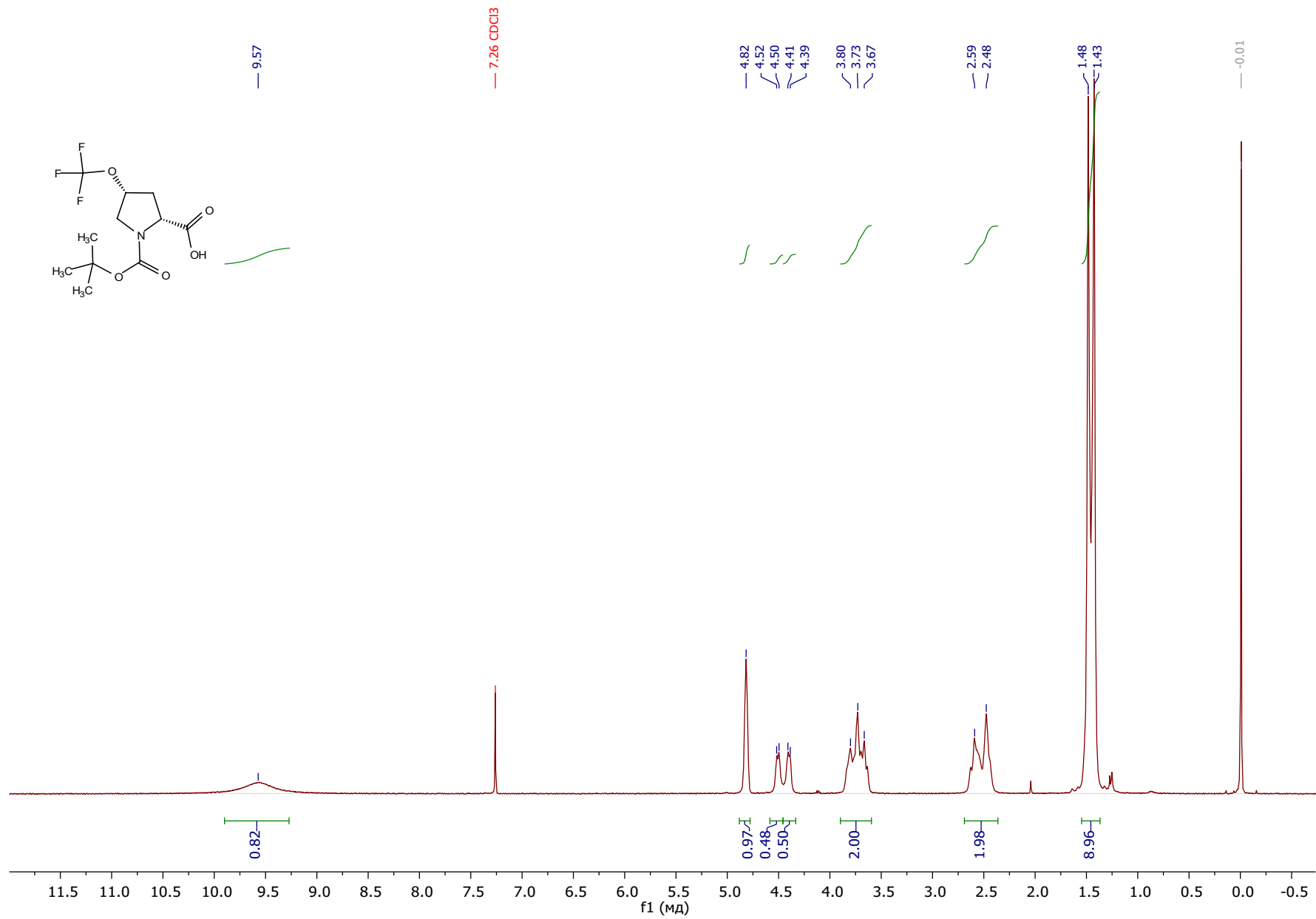


Figure S20. ¹H NMR of Compound (2S,4S)-11 (400 MHz, CDCl₃)

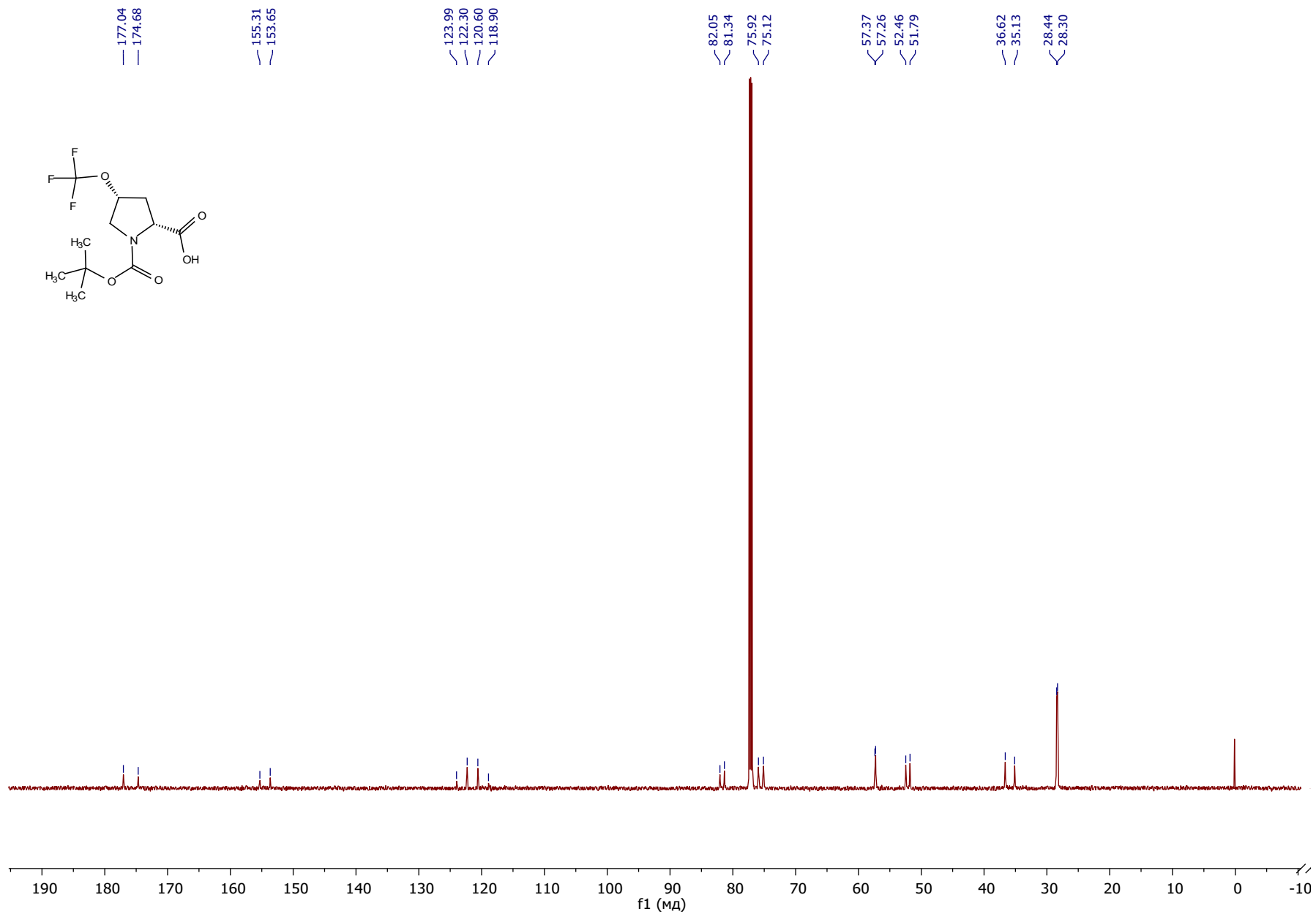


Figure S21. $^{13}\text{C}\{^1\text{H}\}$ NMR of Compound (2S,4S)-11 (151 MHz, CDCl_3)

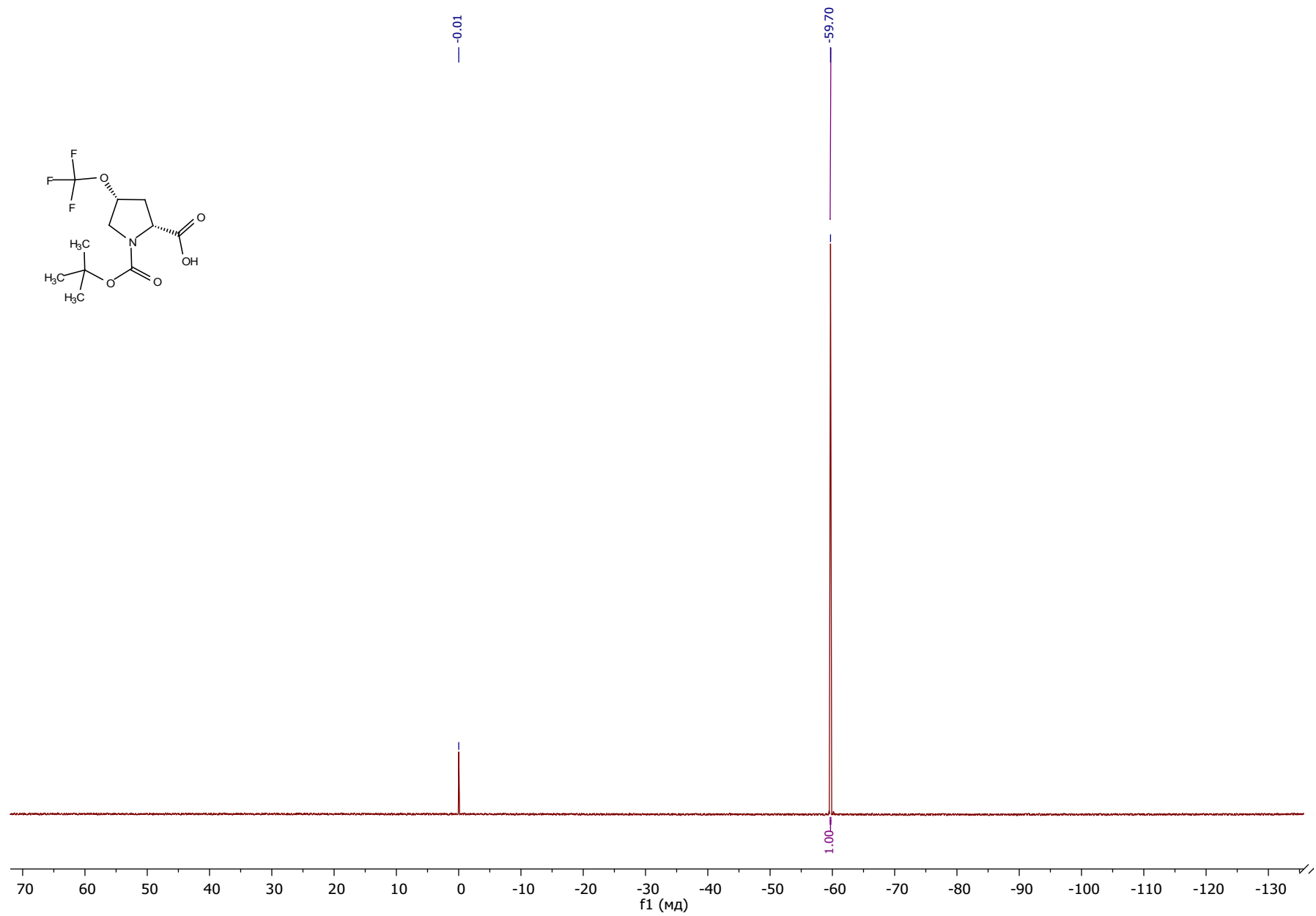


Figure S14. $^{19}\text{F}\{^1\text{H}\}$ NMR of Compound (2S,4S)-11 (376 MHz, CDCl_3)